Pigment Compositions, Spectral Properties, and Energy Transfer Efficiencies between the Xanthophylls and Chlorophylls in the Major and Minor Pigment−Protein Complexes of Photosystem II[†]

Somes Kumar Das and Harry A. Frank*

Department of Chemistry, University of Connecticut, Storrs, Connecticut 06269-3060

Received July 18, 2002; Revised Manuscript Received August 30, 2002

ABSTRACT: Absorption, fluorescence, and fluorescence excitation spectra have been measured from CP26, CP29, and monomeric and trimeric LHCIIb light-harvesting complexes isolated from Photosystem II subchloroplast particles from spinach. The complexes were purified using a combination of isoelectric focusing and sucrose gradient ultracentrifugation. The chlorophyll (Chl) and xanthophyll pigment compositions were measured using high-performance liquid chromatography (HPLC). Using the pigment compositions from the HPLC analysis as a starting point, the absorption spectral profiles of the complexes have been reconstructed from the individual absorption spectra obtained for each of the pigments. Also, the fluorescence excitation spectra of the complexes have been deconvoluted. The data reveal the energy transfer efficiencies between Chl *b* and Chl *a* and between specific xanthophylls and Chl *a* in the complexes. The spectral analyses reveal the underlying features of the highly congested spectral profiles associated with the complexes and are expected to be beneficial to researchers employing spectroscopic methods to investigate the mechanisms of energy transfer between the pigments bound in these complexes.

The light-harvesting apparatus in photosynthetic organisms is comprised of several membrane-bound pigment−protein complexes that absorb photons of light and transfer the energy to the reaction center (*1*−*5*). In higher plants, the light-harvesting assemblies associated with Photosystems I and II (PSI and PSII)[1] are denoted LHCI and LHCII (*6*). LHCII is assembled from the products of the Lhcb genes and consists of four different chlorophyll (Chl)- and xanthophyll-binding pigment−protein complexes known as LHCIIa, LHCIIb, LHCIIc, and LHCIId (*1*, *7*−*9*). LHCIIb is the most abundant and is present in a vast stoichiometric excess over the PSII reaction center. In its native form, it is a trimeric complex and binds over half of the Chl in PSII (*8*, *10*, *11*). LHCIIa, LHCIIc, and LHCIId are familiarly known as the minor Chl *a*/*b* complexes CP29, CP26, and CP24, respectively, based on their apparent molecular weights from nondenaturing SDS−PAGE (*12*−*16*). These minor complexes exist in roughly a 1:1 stoichiometric ratio with the PSII reaction center (*17*).

A structural model of the LHCIIb protein has been obtained from electron microscopic studies (*10*). The model shows the relative positions of 12 Chls and 2 xanthophylls, assigned as luteins in sites denoted L1 and L2, bound to a single polypeptide of 232 amino acids. The structure was not sufficiently resolved to distinguish between Chls *a* and *b*, and the xanthophylls, neoxanthin and violaxanthin, also known to be present in the complex (*11*, *18*), were not observed. The structures of the CP29, CP26, and CP24 complexes have not been solved to atomic resolution, but it is known from biochemical studies that they are between 210 and 257 amino acids in length, bind 6 Chl *a* and between 2 and 4 Chl *b* molecules, and have between 29.2% and 48.7% sequence homology with LHCIIb (*19*). It is also known that there is considerable variability in the xanthophyll composition among these complexes (*1*, *8*, *9*). In particular, the minor complexes are enriched in violaxanthin compared to LHCIIb (*7*, *9*, *20*). Violaxanthin can be reversibly de-epoxidized to antheraxanthin and zeaxanthin in the so-called xanthophyll cycle which has been implicated in the regulation of energy flow in the antenna systems of higher plants and algae (*21*−*24*). Under conditions where light is limiting, the efficiency requirement for light-harvesting is at a maximum, and the violaxanthin content is high. Under high light conditions, de-epoxidation of violaxanthin to zeaxanthin occurs as light-harvesting efficiency is down-regulated. The presence of zeaxanthin has been correlated with nonradiative energy dissipation observed as nonphotochemical quenching (NPQ) of Chl fluorescence (*25*, *26*). Because the majority of the xanthophyll cycle pigments have been found in the minor complexes, the suggestion has been made that the molecular site for NPQ resides within these proteins (*27*). Further

[†] This work has been supported in the laboratory of H.A.F. by the National Science Foundation (MCB-9816759), the National Institutes of Health (GM-30353), and the University of Connecticut Research Foundation.

* To whom correspondence should be addressed. Phone: (860) 486-2844; Fax: (860) 486-6558; E-mail: harry.frank@uconn.edu.

[1] Abbreviations: BSA, bovine serum albumin; Chl, chlorophyll; CP, chlorophyll protein; DM, *n*-dodecyl-*β*-D-maltoside; EDTA, ethylenediaminetetraacetic acid; HEPES, *N*-(2-hydroxyethyl)piperazine-*N*′-2-ethanesulfonic acid; HPLC, high-performance liquid chromatography; IEF, isoelectric focusing; LHC, light-harvesting complex; MES, 2-(*N*-morpholino)ethanesulfonic acid; NPQ, nonphotochemical quenching; PSII, Photosystem II; SDS−PAGE, sodium dodecyl sulfate−polyacrylamide gel electrophoresis.

10.1021/bi0204802 CCC: $22.00
Published on Web 09/27/2002

support for this assignment has emerged from the identification of protonation sites in CP26 and CP29 (*28*−*30*), thought to correspond to the low luminal pH requirement for NPQ, and from the fact that CP29 is reversibly phosphorylated under stress conditions, suggesting an involvement in stress resistance (*31*).

Understanding how the LHCII proteins operate in the roles of light-harvesting and energy flow regulation requires a precise knowledge of the relationship between the pigment composition of the complexes and their photochemical properties. In steady-state absorption and fluorescence excitation spectroscopic studies on light-harvesting pigment−protein complexes prepared from bacterial photosynthetic organisms, the efficiency of energy transfer between the bound carotenoids and the bacteriochlorophylls has been shown to be dependent on the carotenoid composition (*32*, *33*). In those systems, the optical transitions associated with the various bound pigments are spectrally well-resolved, facilitating the assignment of the photochemical properties of individual molecules. This is not the case for the higher plant pigment−protein complexes which exhibit highly congested spectral profiles. The absorption spectral transitions associated with the various pigments in the LHCIIb and the CP complexes overlap significantly in the 400−550 nm visible wavelength region, making it very difficult to correlate the spectral properties of the pigments with their photochemical behavior. Also, because of this overlap, it is very difficult to excite sole xanthophyll molecules and deduce energy transfer efficiencies between them and Chl. Any quantitative evaluation of the spectral properties and energy transfer efficiencies of specific pigments in the complexes will necessarily require some form of spectral deconvolution (*9*, *34*−*38*).

In this work, we have isolated CP26, CP29, and monomeric and trimeric LHCIIb antenna complexes from spinach using a combination of isoelectric focusing (IEF) and sucrose gradient ultracentrifugation and have measured the Chl and xanthophyll pigment compositions of the proteins using high-performance liquid chromatography (HPLC). We have also measured the absorption and fluorescence excitation spectra of the proteins. Using the pigment compositions determined from the HPLC analysis as a starting point, we have reconstructed the absorption spectral profiles of the complexes using the spectral line shapes associated with each of the individual pigments. In addition, we have deconvoluted the fluorescence excitation spectra of the complexes. The data reveal the energy transfer efficiencies between specific xanthophylls and Chl *a* in the complexes. In addition to providing information on light-harvesting by the xanthophylls, the spectral analyses reveal which pigments are absorbing at specific wavelengths. The data are expected to be beneficial to researchers employing steady-state and transient optical spectroscopic methods to investigate the mechanisms of energy transfer between the pigments bound in these complexes (*9*, *34*, *39*−*62*).

MATERIALS AND METHODS

Sample Preparation and Analysis

Thylakoid Membranes. Fresh spinach was dark-adapted for overnight in the cold room. Approximately 500 g of leaves was washed, destemmed, and ground with 400 mL of grinding buffer (0.4 M NaCl, 20 mM HEPES, 4.0 mM $MgCl_2 \cdot 6H_2O$, 5 mM EDTA, 1 mg/mL BSA, pH 7.6, with NaOH) at 4 °C in a blender at a high speed. The ground spinach was filtered through 5−6 layers of cheesecloth, and the filtrate was centrifuged at 6000*g* for 8 min in a Sorvall SS-34 rotor. The pellet was resuspended in wash buffer (0.15 M NaCl, 20 mM HEPES, 4 mM $MgCl_2 \cdot 6H_2O$, 1 mM EDTA, 1 mg/mL BSA, pH 7.6, with NaOH) to a total volume of 120 mL. After a short slow spin of 30 s at 500*g* to sediment the nonchloroplast material, the supernatant was centrifuged for 10 min at 7000*g*. The pellet was collected and resuspended in ethylene glycol (EG) suspension buffer [15 mM NaCl, 20 mM MES, 5 mM $MgCl_2 \cdot 6H_2O$, 1 mM EDTA, 1 mg/mL BSA, 30% EG (v/v), pH 6.0, with NaOH] to ∼80 mL and centrifuged for 10 min at 12000*g*. The last step was repeated and the pellet was resuspended in 20 mL of EG suspension buffer to a chlorophyll concentration not less than 3 mg/mL.

BBY Particles. The subchloroplast BBY particles (*63*) were prepared according to the following procedure. The chlorophyll concentration was measured in assay buffer following the equation: chlorophyll concentration (mg/mL) = [(1.01 × 10^{-2})(OD at 645 nm) + (1.45 × 10^{-2})(OD at 652 nm) + (4.01 × 10^{-3})(OD at 663 nm)]. The volumes of suspension buffer (15 mM NaCl, 20 mM MES, 30% EG, pH 6.0) and Triton X-100 buffer [15 mM NaCl, 20 mM MES, 5 mM $MgCl_2 \cdot 6H_2O$, 1 mM EDTA, 1 mg/mL BSA, 20% (v/v) Triton X-100, a small amount of catalase, pH 6.0 with NaOH] necessary for the next step were calculated from the chlorophyll concentration and the initial volume of the thylakoids from the formulas:

$$\text{suspension buffer (mL)} = [3/8 \times (\text{Chl concn in mg/mL}) - 1] \times (\text{volume of thylakoids in mL})$$

$$\text{Triton X-100 buffer (mL)} = [(\text{Chl concn in mg/mL})/8] \times (\text{volume of thylakoids in mL})$$

The thylakoid membranes were stirred in on ice, and the calculated amount of suspension buffer was added. Then the calculated amount of Triton X-100 buffer was added dropwise and stirred for 20 min in an ice bath in the dark. After the incubation period, the solution was put in centrifuge tubes and centrifuged for 20 min at 37000*g*. The pellet was collected gently with a paintbrush and resuspended in a minimal amount of suspension buffer. The chlorophyll concentration was determined following the same equation mentioned above. Again, the amount of suspension buffer and the Triton X-100 buffer to be added in the next step were calculated using the equations:

$$\text{suspension buffer (mL)} = [19/40 \times (\text{Chl concn in mg/mL}) - 1] \times (\text{volume of thylakoids in mL})$$

$$\text{Triton X-100 buffer (mL)} = [(\text{Chl concn in mg/mL})/40] \times (\text{volume of thylakoids in mL})$$

These were added to the sample by the same procedure as before without the final incubation. The solution was

poured into 50 mL centrifuge tubes and centrifuged for 20 min at 39000*g*. The supernatant was discarded, and the pellet was resuspended in suspension buffer. The total volume after suspension was 2 times the total volume of sample and buffer in the previous step. Again, the solution was centrifuged for 20 min at 39000*g*. The collected pellet consisted of BBY particles which were used in the preparation of major and minor LHCII light-harvesting complexes.

Fractionation of BBY Particles by Sucrose Density Gradient Centrifugation. BBY particles were washed in 1 mM EDTA, pH 8.0, then suspended in water at 2 mg of chlorophyll/mL, and solubilized by adding an equal volume of 2% *n*-dodecyl-*β*-D-maltoside (DM, Calbiochem) in water. The solubilized sample was spun for 2 min at 10000*g* at 4 °C and rapidly loaded onto a continuous sucrose density gradient prepared by freezing and thawing a 0.5 M sucrose solution containing 10 mM HEPES, pH 7.6, and 0.06% DM. The gradient was then spun in a Beckman SW40 rotor at 285000*g* for 23 h at 4 °C. The second band containing the CP complexes and monomers of LHCIIb and the third band containing the LHCIIb trimers were harvested carefully with a syringe.

Isoelectric Focusing. The LHCIIb and CP complexes were separated by nondenaturating isoelectric focusing (IEF) using procedures similar to those previously described (*17*, *64*). A slurry of volume 100 mL containing 4% Ultrodex, 2% Ampholine carrier ampholites (pH 3.5−5.0), 1% glycine, and 0.06% DM was prepared. The IEF electrode strips were cut into six 10.5 cm lengths, soaked in a 2% Ampholine solution, and placed in the 26.0 × 11.0 cm tray of a Pharmacia Multiphore II Electrophoresis system. The slurry was poured into the tray to form a homogeneous layer. After carefully removing the air bubbles, the tray was placed 100 cm below a small fan on a balance to allow control of the weight of the evaporated water; 15 g of water was evaporated in nearly 2 h. The tray with prepared gel was placed onto the cooling plate (cooled to 4 °C) and was focused for ∼1.0 h at 8.0 W. A film of water containing a nonionic detergent (e.g., 0.1% Triton X-100) was used to aid thermal conductivity.

Freshly prepared PSII antenna complexes from the sucrose density gradient centrifugation step (∼1.0 mL) having a total chlorophyll concentration of 5.0 mg/mL were mixed with 1 mL of deionized water and 0.5 mL of 3% DM. The sample was kept on ice and occasionally stirred for 30 min. The final chlorophyll concentration was ∼2.0 mg/mL. The sample was centrifuged at 39000*g*, and the supernatant (∼2.0 mL) was applied 2 cm from the cathode to the precooled and prefocused gel using a 10 × 2 cm sample applicator. To apply the sample, the applicator was pressed through the gel bed at the desired position. The gel inside the applicator was scraped out and mixed with the prepared sample. The gel slurry with the sample was poured back into the applicator, the applicator was removed, and the bed was allowed to equilibrate hydrostatically for 3 min. The electrode holder with the IEF electrodes was placed onto the electrode strips to start the focusing. The focusing procedure was continued for 15 h at a constant power of 8.0 W at 4 °C. The initial and the final current values were normally 13 and 5 mA, respectively. After the completion of the focusing, a small amount of gel from each of the green bands was dissolved in 1 mL of deionized water, and the pH was measured using a microelectrode. Each green band in the gel was separated using the fractionating grid frame and was collected by a spatula. The sample was eluted using columns with a minimum volume of a solution containing 100 mM HEPES (pH 7.6) and 0.06% DM. The p*I* values for the LHCIIb, CP26, and CP29 complexes were 4.12, 4.45, and 4.68, respectively. The uncertainties in these values are ±0.04 on the gel.

Ultracentrifugation. The samples were further purified by ultracentrifugation on a continuous sucrose density gradient prepared by freezing and thawing a 0.5 M sucrose solution containing 10 mM HEPES, 0.06% DM at pH 7.6. The run was for 18−20 h at 285000*g* in an SW40 rotor at 4 °C.

SDS−PAGE. SDS−PAGE was performed in a Hoefer SE600 vertical electrophoresis unit (Amersham Pharmecia Biotech) with a 1.5 mm thick slab gel using 14% total acrylamide and bisacrylamide (denoted T) and 3% of the cross-linker, bisacrylamide (denoted C), calculated from the formulas:

$$\%\,T = [(\text{acrylamide} + \text{bisacrylamide})\ \text{in grams} \times 100]/100\ \text{mL}$$

$$\%\,C = [(\text{bisacrylamide})\ \text{in grams} \times 100]/[(\text{acrylamide} + \text{bisacrylamide})\ \text{in grams}]$$

as a uniform separating gel overlaid by a 4% T, 3% C, 2 cm stacking gel. The separating gel solution contained 14% acrylamide, 11% sucrose, 0.04% TEMED in 1 M Tris, at pH 8.4. The stacking gel solution contained 4% acrylamide and 0.005% TEMED in 0.74 M Tris, pH 8.4. The gels were polymerized together, without prior degassing, by adding 0.05% ammonium persulfate. Sucrose in the separating gel solution prohibits mixing with the stacking gel solution during polymerization. The Tris−Tricine buffer system was that described by Schägger and Von Jagow (*65*): anode buffer, 0.2 M Tris, pH 8.9; cathode buffer, 0.1 M Tris, 0.1 M Tricine, 0.1% SDS, 1 mM EDTA, pH 8.2. Samples containing 5 μg of chlorophyll were denatured in a buffer containing 2% SDS, 60 mM Tris, pH 6.8, 10% glycerol, 2% mercaptoethanol, and 0.05% (w/v) bromophenol blue, by placing them in boiling water for 2 min. Afterward, 30 μL of solution was placed in each channel of the gel. The gels were run at a constant current of 30 mA at 4 °C. Apparent molar masses were estimated using the markers phosphorylase *b* (94 kDa), albumin (67 kDa), ovalbumin (43 kDa), carbonic anhydrase (30 kDa), trypsin inhibitor (20.1 kDa), and α-lactalbumin (14.4 kDa). The gels were stained for 6 h in 30% methanol, 10% acetic acid, 0.1% Coomassie brilliant Blue (R-350), and then destained with a solution containing 16% methanol, 7% acetic acid in distilled water. A typical result is shown in Figure 1.

Pigment Analysis. The Chl *a*, Chl *b*, and xanthophyll compositions of the different chlorophyll−protein complexes were obtained from HPLC analysis. A sample chromatogram from the pigment extract of LHCIIb is shown in Figure 2. Samples of approximately 0.1 mL were dissolved in 1:1 methanol and acetone (v/v), and the pigments were extracted after careful homogenization. The extracts were injected into a Millipore Waters 600E HPLC using a Nova-Pak C18 column employing solvents A = acetone, B = methanol, and C = water in the mobile phase. The run was programmed as follows: 0−10 min, isocratic 58% acetone/17% methanol/

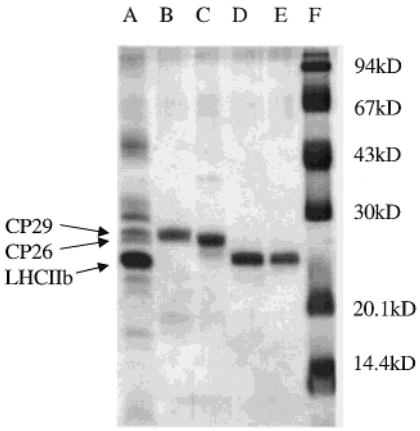

FIGURE 1: SDS−PAGE revealing the polypeptide composition of the pigment−protein complexes used in the spectroscopic experiments. The lanes are as follows: A, BBY particles; B, CP29; C, CP26; D, LHCIIb monomers; E, LHCIIb trimers; F, molecular mass standards. The details of the buffer system and procedure are described under Materials and Methods.

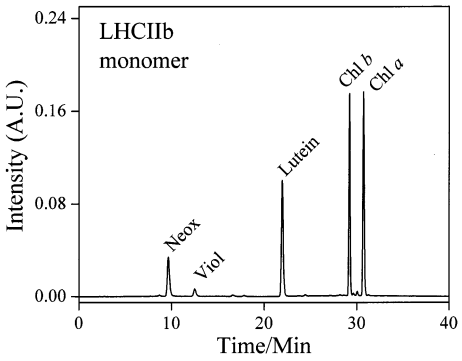

FIGURE 2: HPLC analysis of the pigments extracted from the LHCIIb complex showing baseline separation between peaks. The relative compositions of the pigments in the complexes were obtained by comparing the areas under the chromatographic peaks with area vs concentration calibration curves constructed from control HPLC runs using different concentrations of the purified pigments.

25% water; 10−20 min, linear gradient to 60% acetone/20% methanol/20% water; 20−50 min, linear gradient to 75% acetone/20% methanol/5% water. The eluent was monitored using the single diode array detector, and the fractions were identified by their absorption spectra recorded separately in the similar solvent compositions. The relative compositions of the pigments in the complexes were computed by comparing the areas under the chromatographic peaks of the extracts with area vs concentration calibration curves constructed from control experiments where different concentrations of the purified pigments were injected into the HPLC. The solvents were acetone (99.6%), methanol (99.9%), and distilled water from Fisher, and ethanol (100%) from AAPER.

Absorption and Fluorescence Spectroscopic Measurements

The spectroscopic experiments were carried out at room temperature unless otherwise noted. Absorption spectra were recorded at room temperature using a Milton Roy Spectronic 3000 Array photodiode array spectrometer. Fluorescence spectroscopy was carried out at 12 °C using an SLM Instruments, Inc., model 8000C spectrofluorometer employing a 450 W ozone-free xenon arc lamp and a monochromator with a grating having 1500 grooves/mm for excitation. The sample emission passed through a 665 nm cut-off filter, and into another monochromator positioned 90° to the excitation beam. For fluorescence excitation spectroscopy, the spectral profile of the incident light was monitored using 1,1′,3,3,3′,3′-hexamethylindotricarbocyanine perchlorate (HITC) in acetonitrile (0.5 g/100 mL) as a quantum counter (*66*). The emission and incident light were detected by two independent Hamamatsu model R-928 photomultiplier tubes. Fluorescence spectra were corrected for the wavelength dependences of the optical components using a correction factor generated by a Spectral Irradiance 45 W quartz−halogen tungsten-coiled filament lamp standard. The concentration of the samples was kept below 10^{-6} M, which corresponds to an optical density at 680 nm less than 0.05. All spectral analyses including addition, subtraction, multiplication, differentiation, and integration were done using Origin version 6.0 software (*67*).

RESULTS AND DISCUSSION

Pigment Compositions

The pigment compositions of the CP26, CP29, and monomeric and trimeric LHCIIb complexes determined by HPLC (e.g., see Figure 2) are given in Table 1. The results are presented as relative molar amounts with respect to Chl *a*. In agreement with previous findings (*7*, *17*, *20*, *68*), the data in Table 1 show that the proportion of Chl *b* is a maximum in LHCIIb, less in CP26, and a minimum in CP29. Lutein and neoxanthin are present in maximum proportions in LHCIIb compared to the other complexes. Also, in agreement with previous findings, violaxanthin is found in higher amounts in the minor complexes than in the LHCIIb complex. Small discrepancies between the present data and the previously reported results (summarized in Table 1) may be attributed to differences in the growth conditions of the plants, different extents of dark-adaptation, or the methods of purification of the complexes. Although the IEF procedures for the purification of the complexes used here were similar to those previously published (*17*, *64*), redistribution in pigment composition may occur during thylakoid fractionation with Triton X-100 (*69*). It is also important to note that the various pigments have different binding affinities (*68*) that may affect the extent to which they are retained during the preparation of the complexes. The binding affinity is in the following order from strongest to weakest: Chl *b* > neoxanthin > Chl *a* > lutein > zeaxanthin > violaxanthin (*68*). The absence of any detectable amounts of zeaxanthin in these complexes is suggestive of its nearly complete conversion to violaxanthin in the dark-adapted spinach from which all the complexes were prepared and/or its removal from the complexes during detergent treatment and purification.

Spectroscopic Measurements

Absorption Spectroscopy. Figure 3 shows the absorption spectra in the region 400−700 nm of the LHCIIb trimer, LHCIIb monomer, CP26, and CP29 antenna complexes suspended in 100 mM HEPES (pH 7.6) buffer containing 0.06% DM. The absorption spectra differ primarily in the

Table 1: Pigment Composition Expressed in Molar Amounts Relative to Chl *a* of the LHCIIb Trimer, LHCIIb Monomer, CP26, and CP29 Light-Harvesting Complexes Associated with PSII

complex	source	Chl *a*	Chl *b*	lutein	neoxanthin	violaxanthin	Chl *a*/ Chl *b*	method	reference
LHCIIb	spinach	1.00	0.78 ± 0.06	0.25 ± 0.04	0.12 ± 0.03	0.03 ± 0.01	1.28	HPLC	this work
(trimer)	spinach		0.80 ± 0.05	0.23 ± 0.04	0.08 ± 0.03	0.03 ± 0.01	1.25	spectral decon	this work
	spinach		0.72 ± 0.05	0.22 ± 0.03	0.11 ± 0.02	0.025 ± 0.004	1.38	HPLC	(*9*)
	spinach		0.75	0.28	0.15	0.03	1.33	HPLC	(*68*)
	barley		0.75	0.25	0.125	0.062	1.33	HPLC	(*7*)
LHCIIb	spinach	1.00	0.75 ± 0.05	0.22 ± 0.04	0.10 ± 0.03	0.04 ± 0.02	1.33	HPLC	this work
(monomer)	spinach		0.77 ± 0.04	0.24 ± 0.03	0.08 ± 0.02	0.03 ± 0.01	1.29	spectral decon	this work
	spinach		0.88 ± 0.04	0.26 ± 0.03	0.11 ± 0.02	0.01 ± 0.005	1.14	HPLC	(*9*)
	barley		0.75	0.25	0.125	0.062	1.33	HPLC	(*7*)
	Zea-mays		0.74	0.24	0.062	0.01	1.36	HPLC	(*20*)
CP26	spinach	1.00	0.44 ± 0.04	0.19 ± 0.04	0.06 ± 0.02	0.08 ± 0.02	2.27	HPLC	this work
(LHCIIc)	spinach		0.48 ± 0.05	0.15 ± 0.03	0.08 ± 0.02	0.06 ± 0.02	2.08	spectral decon	this work
	spinach		0.40	0.16	0.13	0.12	2.50	HPLC	(*68*)
	barley		0.57	0.28	0.14	0.07	1.75	HPLC	(*7*)
	Zea-mays		0.52	0.23	0.054	0.087	1.92	HPLC	(*20*)
CP29	spinach	1.00	0.33 ± 0.04	0.23 ± 0.04	0.05 ± 0.02	0.10 ± 0.02	3.03	HPLC	this work
(LHCIIa)	spinach		0.40 ± 0.06	0.20 ± 0.05	0.08 ± 0.02	0.10 ± 0.02	2.50	spectral decon	this work
	spinach		0.29	0.13	0.09	0.18	3.45	HPLC	(*68*)
	barley		0.44	0.22	0.11	0.22	2.27	HPLC	(*7*)
	Zea-mays		0.39	0.21	0.074	0.14	2.57	HPLC	(*20*)

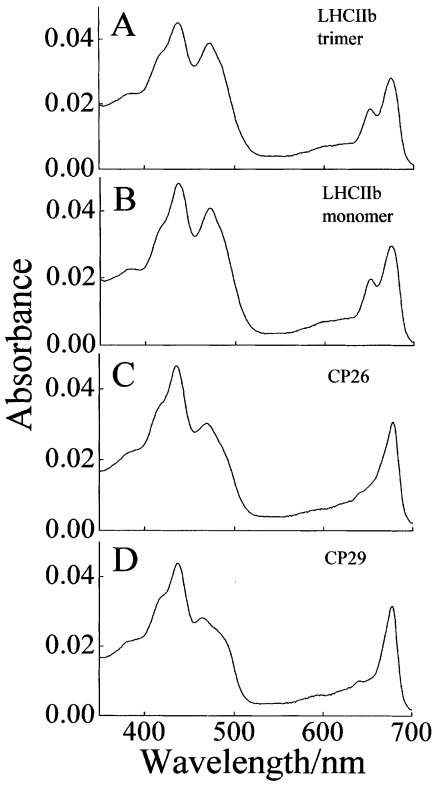

FIGURE 3: Absorption spectra of (A) LHCIIb trimers, (B) LHCIIb monomers, (C) CP26, and (D) CP29 light-harvesting complexes recorded in 100 mM HEPES (pH 7.6) containing 0.06% DM at room temperature.

Chl *b* Soret/xanthophyll region (450−500 nm) and in the Chl *b* Q_y region near 645 nm, consistent with differences in the pigment composition among the complexes (Table 1). The characteristic trends are as follows: (i) There is an decrease in the intensity of the prominent Chl *b* Soret peak at ~472 nm in the order LHCIIb > CP26 > CP29. (ii) There is a decrease in the intensity of the Chl *b* Q_y band at approximately 650 nm in the same order, LHCIIb > CP26 > CP29. (iii) In the region 450−500 nm, there is a gradual broadening of the spectral profile in going from LHCIIb to CP26 to CP29. These trends are indicative of lesser relative amounts of Chl *b* and increased relative amounts and a more even distribution of the various xanthophylls in the minor complexes, especially in CP29 compared to LHCIIb.

Deconvolution of Absorption Spectra. One goal of the present study is to deconvolute the absorption profiles of the complexes to reveal the spectral features associated with each of the bound pigments. The absorption region between 630 and 720 nm associated with the Chl *a* and Chl *b* Q_y transitions in these complexes has already been spectrally deconvoluted and discussed in great detail by previous workers (*35*, *36*, *70*). The results show that the absorption features in this wavelength region can be understood by linear combinations of very similar sets of Gaussian bands for all the complexes. This suggests that the spectra in this region are inhomogeneously broadened either by differences in the energies of the chromophore binding sites or by differences in the distribution of protein conformational states. Here we focus on the region of the Chl *a* and Chl *b* Soret and xanthophyll transitions from 400 to 530 nm (Figure 4). The solid lines are the experimentally observed absorption spectra from the complexes suspended in buffer. The long dashed lines are spectral profiles corresponding to Chl *a* in the protein, and the dotted lines correspond to the absorption spectra of Chl *b* in the protein. These spectral line shapes were obtained from the difference between the absorption spectra of fully reconstituted recombinant LHCII antenna proteins and those missing individual Chl pigments (*37*). For the absorption spectra from all the samples, the xanthophyll plus Chl line shapes were constructed from a sum of the absorption spectra of Chl *a*, Chl *b*, lutein, neoxanthin, and violaxanthin, first taking into consideration the pigment composition of the samples revealed by the HPLC analysis (Table 1) and then allowing further small variations in composition to render the constructed absorption line shapes consistent with the experimental absorption spectra. For the monomeric and trimeric LHCIIb and for CP26, two Chl *a* and three Chl *b* spectra were required to obtain good agreement between the computed and experimental line shapes. For the CP29 absorption spectra, two Chl *a* and two

Table 2: The Peak Maxima of the Chls and Xanthophylls in the Reconstructed Absorption Spectra of the Protein Complexes[a]

protein complex	Chl *a* Soret (nm)	Chl *b* Soret (nm)	lutein (nm)	neoxanthin (nm)	violaxanthin (nm)
LHCIIb (trimer)	439 (Chl *a*1) 432 (Chl *a*2)	483 (Chl *b*1) 476 (Chl *b*2) 467 (Chl *b*3)	500, 472, 450 (L1) 495, 467, 445 (L2)	491, 462, 447	491, 460, 438
LHCIIb (monomer)	439 (Chl *a*1) 432 (Chl *a*2)	483 (Chl *b*1) 476 (Chl *b*2) 467 (Chl *b*3)	499, 471, 449 (L1) 494, 466, 444 (L2)	491, 462, 447	491, 460,438
CP26	439 (Chl *a*1) 431 (Chl *a*2)	482 (Chl *b*1) 477 (Chl *b*2) 464 (Chl *b*3)	498, 470, 448	490, 461, 446	493, 463, 440
CP29	439 (Chl *a*1) 432 (Chl *a*2)	477 (Chl *b*1) 463 (Chl *b*2)	495, 467, 445	489, 460, 445	490, 460, 437

[a] The uncertainties in the peak positions are approximately ±2 nm based on the variation in the goodness-of-fits of the computed spectra.

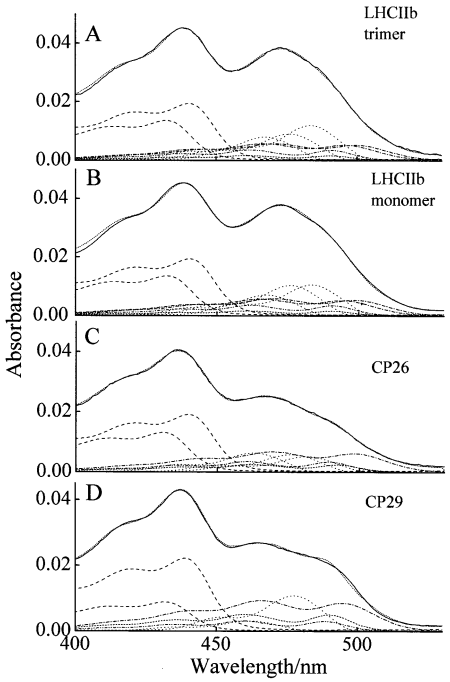

FIGURE 4: Reconstruction of the room-temperature absorption spectra from (A) LHCIIb trimers, (B) LHCIIb monomers, (C) CP26, and (D) CP29 light-harvesting complexes in the Soret and xanthophyll absorption region from 400 to 530 nm. The solid lines correspond to the experimental absorption spectra of the complexes. The dashed lines correspond to the absorption spectra of Chl *a* in Lhc protein. The dotted lines correspond to the absorption spectra in the Soret region of Chl *b* in the protein. The peak maxima used for the Soret band of two Chls *a* were 431 ± 1 and 439 ± 1 nm, and for three Chls *b* were 465 ± 1, 476 ± 1, and 481 ± 1 nm to account for the small effect of environment on the Chl peak positions and to align the spectra better with the absorption maxima of the complexes. The overall absorption line shape used for each form of Chl *a* or Chl *b* was the same. The dashed/dotted lines represent the absorption spectra for lutein taken in ethanol and shifted by between 18 and 22 nm to accommodate the large spectral shift associated with the change in polarizability of the medium. Similarly dashed/double-dotted and short dashed lines represent the absorption spectra for neoxanthin and violaxanthin, respectively. The short dotted lines are simulations of the experimental line shapes generated by summing the absorption spectra of Chl *a*, Chl *b*, and xanthophylls in the amounts represented in the figure.

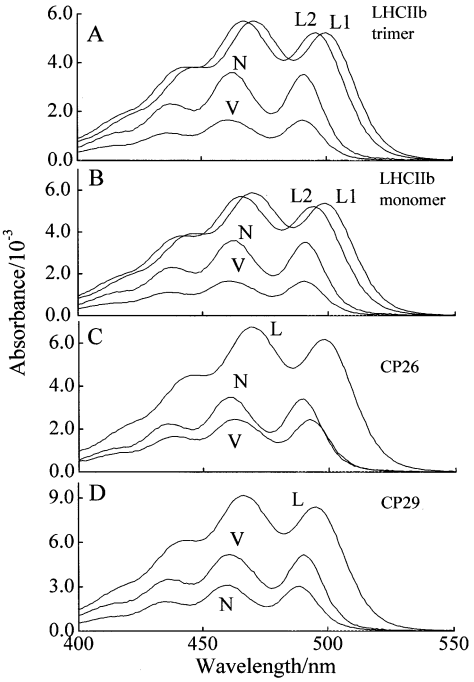

FIGURE 5: Expansion of the scale of Figure 4 showing only the spectra of the xanthophylls used to fit the experimental spectra of the light-harvesting complexes. L1 and L2 refer to lutein molecules, and N and V refer to neoxanthin and violaxanthin, respectively.

Chl *b* spectra were needed. The bandwidths of these component spectra were held constant, but they were shifted in wavelength to account for the different environments of the Chl pigments in these complexes. The combination dashed/dotted or small dashed lines represent the absorption spectra of the various xanthophylls taken in ethanol and shifted by between 18 and 22 nm to accommodate the large spectral shift associated with the change in polarizability of the medium (*71*, *72*). No changes in the overall line shapes of the spectra of the xanthophylls were required to simulate the absorption profiles of the complexes. This is consistent with previous work which has shown that for xanthophylls lacking carbonyl functional groups, little effect on the width or vibronic structure is associated with changes in solvent environment (*72*). The peak positions needed to reproduce the experimental spectra are summarized in Table 2.

For the LHCIIb complexes, two different lutein spectra separated by ~5 nm were used to reproduce the absorption spectrum shown in Figure 4. This result is in agreement with findings (*73*) that the two luteins in the binding sites, L1 and L2, of the LHCIIb protein are occupying separate protein environments having different polarizabilities. The notation of L1 and L2 on the spectra in Figures 5 and 8 is based solely on the assignment by Croce et al. (*73*) of these spectra to luteins in specific protein binding sites. For the CP

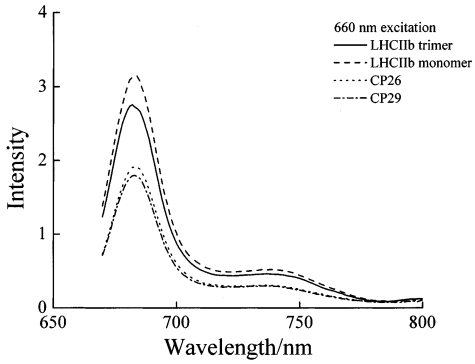

FIGURE 6: Instrument-corrected emission spectra of the light-harvesting complexes, LHCIIb trimers (solid line), LHCIIb monomers (dash), CP26 (short dash), and CP29 (dash/dot) were taken in 100 mM HEPES (pH 7.6) containing 0.06% DM using 660 nm excitation. The intensities of the bands were normalized in the figure to the value of absorption of the sample at the excitation wavelength.

complexes, only one lutein was needed to fit the absorption spectra (Figure 4C,D). Attempts to reconstruct the absorption spectra of the complexes using lesser numbers of component spectra of Chl *a* or *b* were unsuccessful (data not shown). Computed spectra derived from multiple Chl *a* and *b* line shapes are consistent with the pigment compositions determined by HPLC and provide good fits to the experimental spectral line shapes. The stoichiometric ratios of Chl *a*, Chl *b*, and xanthophylls deduced from reconstructing the absorption spectra shown in Figure 4 are given in Table 1. The wavelengths of the peaks associated with the individual pigments giving rise to the absorption spectral line shapes are summarized in Table 2. The data are consistent with the stoichiometries of the complexes previously determined by other workers (*7*, *19*, *20*, *68*, *74*). Second derivatives of the absorption line shapes were also used to test the goodness of fit (data not shown). Using these criteria, excellent agreement was indicated between the experimental and computed spectra.

Emission Spectroscopy. Upon excitation at 620, 630, 650, or 660 nm, all of the samples display a prominent emission peak at 682 ± 1 nm. This peak corresponds to the spectral origin and maximum in the emission spectrum of Chl *a* (*13*, *75*). Figure 6 shows the instrument-corrected emission spectra from all the complexes excited at 660 nm. A lower energy vibronic band occurs in the emission profile at ~740 nm. The emission spectra of the complexes show no dependence in their bandwidth or band maximum on excitation wavelength, but they do differ in their relative emission intensities with excitation in the range 430−500 nm. This is due to the fact that the complexes have different absorbances of the Chl *a*, Chl *b*, and xanthophyll constituent pigments in this wavelength range as well as different efficiencies of energy transfer from the xanthophylls to Chl *a* (see below). Chl *b* emission is usually not detected in steady-state fluorescence experiments on highly purified complexes owing to the rapid and efficient transfer of energy from Chl *b* to Chl *a*. The absence of Chl *b* emission in all the antenna complexes indicates that the efficiency of energy transfer from Chl *b* to Chl *a* is very high.

Quantum Yields. The fluorescence quantum yields of the complexes were measured by integrating the spectra shown in Figure 6. The values were calculated relative to the quantum yield of Rhodamine 800 in methanol, which is known to be 0.086 (*76*). The evaluation of the quantum yields is based on the equation:

$$\phi_f = \phi_r \frac{D_f I_{r\lambda} A_{r\lambda} n_f^2}{D_r I_{f\lambda} A_{f\lambda} n_r^2} \quad (1)$$

where ϕ_f is the fluorescence quantum yield, D_f is the intensity of the excitation beam at wavelength λ, $I_{f\lambda}$ is the optical density at wavelength λ, and $A_{f\lambda}$ is the integrated area of the corrected emission spectrum (*77*). ϕ_r, D_r, $I_{r\lambda}$, and $A_{r\lambda}$ are the corresponding quantities for the rhodamine reference. n_f and n_r are the refractive indexes of HEPES buffer, assumed identical to that of water and ethanol, respectively.

The quantum yields of fluorescence were determined to be 0.085 ± 0.005, 0.096 ± 0.005, 0.058 ± 0.005, and 0.055 ± 0.005 for the LHCIIb trimer, LHCIIb monomer, CP26, and CP29 complexes, respectively. There are many factors that could account for the fact that CP26 and CP29 have comparable fluorescence yields with both of these being lower than those from the LHCIIb complexes. These include differences in structure, pigment composition, and/or aggregation state. The lower quantum yield of LHCIIb trimers compared to the LHCIIb monomers has been attributable to the aggregated nature of the trimeric protein preparation (*78*).

Deconvolution of Excitation Spectra. The excitation spectra in the region of the Chl Soret and xanthophylls absorption bands are shown in Figure 7 (solid lines). These

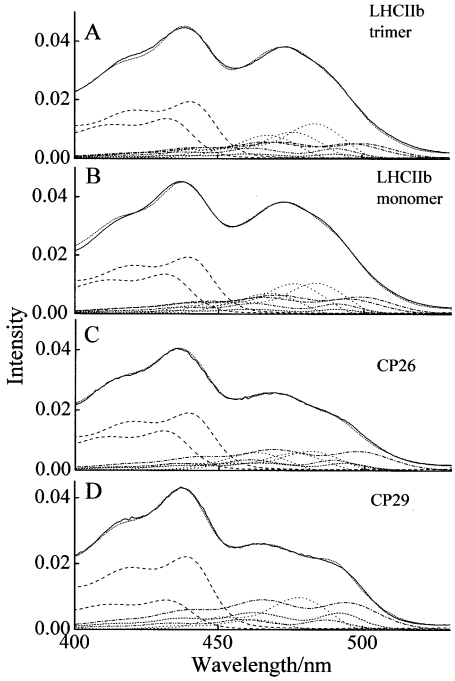

FIGURE 7: Reconstruction of the room-temperature excitation spectra from (A) LHCIIb trimers, (B) LHCIIb monomers, (C) CP26, and (D) CP29 light-harvesting complexes in the Soret and xanthophyll absorption region from 400 to 530 nm. The solid lines correspond to the experimental excitation (A−D) spectra of the complexes. The dashed lines correspond to the excitation spectra of purified Chl *a* in ethanol. The dotted lines correspond to the excitation spectra in the Soret region of purified Chl *b* in ethanol. The dashed/dotted lines represent the absorption spectra for the various xanthophylls taken in ethanol. The details given in the legend of Figure 4 describing the procedure for fitting the absorption spectra also pertain here.

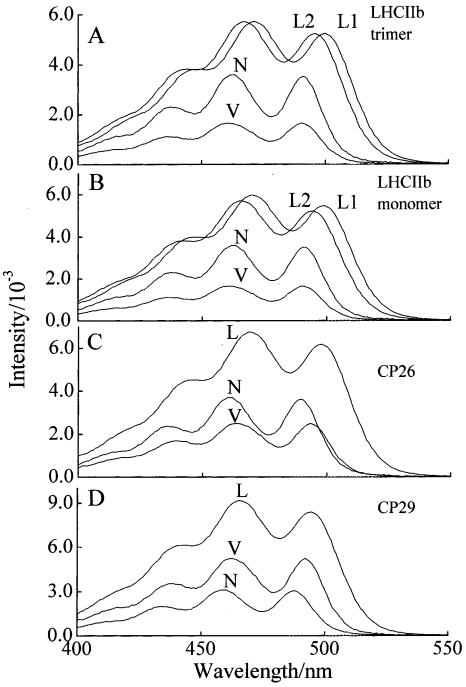

FIGURE 8: Expansion of the scale of Figure 7 showing only the spectra of the xanthophylls used to fit the experimental spectra of the light-harvesting complexes. L1 and L2 refer to lutein molecules, and N and V refer to neoxanthin and violaxanthin, respectively.

spectra were measured by monitoring the Chl *a* emission at 680 nm for all the complexes. The deconvolution of the excitation spectra followed the same procedure as described above for the absorption spectra. The contribution of each pigment to the overall spectral line shape was initially assigned based on the values used for the absorption spectral analysis. Using these as the starting points, adjustments in the component intensities were made to render the computed excitation spectra consistent with the experimental spectra. These final adjustments in the excitation spectra were critical in revealing the energy transfer efficiencies of the pigments to Chl *a*. Figure 8 is presented as an expansion of the scale given in Figure 7 to reveal more clearly the spectra of the xanthophylls. In all cases, the spectra of the constituent Chl *a*, Chl *b*, and xanthophylls were shifted by the same amount as was needed to generate the absorption spectra.

Energy Transfer Efficiencies. By comparing the integrated areas of the Chl *b* and xanthophyll bands in the absorption and excitation spectra, the efficiencies of energy transfer between these pigments and Chl *a* can be calculated. The concentrations of the samples were kept very low (OD $\sim$ 0.05) to ensure a linear relationship between absorbance and excitation intensity. Because the emission from the LHCII complexes at $\sim$681 nm (Figure 6) derives essentially entirely from Chl *a*, only the energy transfer efficiencies to that pigment may be determined from these experiments. The absorption and excitation spectra shown in Figures 4 and 7 were normalized to the integrated area of the Chl *a* spectral line shapes. Comparing the integrated areas of the absorption and excitation line shapes revealed 95 $\pm$ 5% efficiency of energy transfer between Chl *b* and Chl *a* in all the complexes. A similar analysis using the line shapes of the xanthophylls shown in Figures 5 and 8 revealed values of 90 $\pm$ 10% for the efficiencies of energy transfer between all the xanthophyll molecules and Chl *a*. The present work and previous steady-state and dynamic spectroscopic investigations of xanthophylls bound in the central protein binding sites of native and recombinant pigment−protein complexes have not revealed significant differences in the energy transfer efficiencies among xanthophylls (*73*, *79*, *80*). Thus, a change in the structure or excited state energy of a xanthophyll does not lead automatically to an alteration in light-harvesting efficiency.

In summary, the studies reported here have done the following: (1) revealed the Chl and xanthophyll pigment compositions of the proteins from HPLC analysis; (2) reconstructed the absorption and fluorescence spectral profiles of the complexes using the line shapes associated with each of the individual pigments and the pigment compositions determined by HPLC; (3) deconvoluted the fluorescence excitation spectra of the complexes to reveal the energy transfer efficiencies between Chl *b* and Chl *a* and between specific xanthophylls and Chl *a* in the complexes. Data from previous studies have also been summarized and should provide a useful resource for researchers employing spectroscopic methods to investigate the mechanisms of energy transfer between the pigments bound in these complexes.

ACKNOWLEDGMENT

We thank Drs. Gary Brudvig and K. V. Lakshmi for useful discussions and for providing the details of the procedure for the preparation of the BBY particles described in this work. We also thank Professor Robert DeLevie for his advice on the numerical techniques for deconvolution of the spectra, and Drs. Roberta Croce and Roberto Bassi for providing the spectral line shapes of Chl *a* and *b* in the proteins and for useful discussions.

REFERENCES

1. Jansson, S. (1994) *Biochim. Biophys. Acta 1184*, 1−19.
2. Paulsen, H. (1995) *Photochem. Photobiol. 62*, 367−382.
3. Bassi, R., Giuffra, E., Croce, R., Dainese, P., and Bergantino, E. (1996) in *Light as Energy Source and Information Carrier in Plant Physiology. Proceedings of the NATO Advanced Study Institute* (Jennings, R. C., Ed.) pp 41−64, Plenum Press, New York.
4. Green, B. R., and Durnford, D. G. (1996) *Annu. Rev. Plant Physiol. Plant Mol. Biol 47*, 685−714.
5. Pichersky, E., and Jansson, S. (1996) in *Oxygenic Photosynthesis: The light reactions* (Ort, D. R., and Yocum, C. F., Eds.) pp 507−521, Kluwer Academic Publishers, Dordrecht.
6. Thornber, J. P., Peter, G. F., and Nechushtai, R. (1987) *Physiol. Plant. 71*, 236−240.
7. Peter, G. F., and Thornber, J. P. (1991) *J. Biol. Chem. 266*, 16745−16754.
8. Horton, P., Ruban, A. V., and Young, A. J. (1999) in *The Photochemistry of Carotenoids* (Frank, H. A., Young, A. J., Britton, G., and Cogdell, R. J., Eds.) pp 271−291, Kluwer Academic Publishers, Dordrecht.
9. Peterman, E. J. G., Gradinaru, C. C., Calkoen, F., Borst, J. C., van Grondelle, R., and van Amerongen, H. (1997) *Biochemistry 36*, 12208−12215.
10. Kühlbrandt, W., Wang, D. N., and Fujiyoshi, Y. (1994) *Nature 367*, 614−621.
11. Croce, R., Weiss, S., and Bassi, R. (1999) *J. Biol. Chem. 274*, 29613−29623.
12. Thornber, J. P., Peter, G. F., Morishige, D. T., Gomez, S., Anandan, S., Welty, B. A., Lee, A., Kerfeld, C., Takeuchi, T., and Preiss, S. (1993) *Biochem. Soc. Trans. 21*, 15−18.
13. Bassi, R., Rigoni, F., Barbato, R., and Giacometti, G. M. (1987) *J. Biol. Chem. 262*, 13333−13341.
14. Green, B. R. (1988) *Photosynth. Res. 15*, 3−32.
15. Boekema, E. J. G., van Roon, H., van Breemen, J. F. L., and Dekker, J. P. (1999) *Eur. J. Biochem. 266*, 444.

16. Pascal, A., Gradinaru, C., Wacker, U., Peterman, E., Calkoen, F., Irrgang, K.-D., Horton, P., Renger, G., Van Grondelle, R., Robert, B., and Van Amerongen, H. (1999) *Eur. J. Biochem. 262*, 817−823.
17. Ruban, A. V., Young, A. J., Pascal, A. A., and Horton, P. (1994) *Plant Physiol. 104*, 227−234.
18. Croce, R., Remelli, R., Varotto, C., Breton, J., and Bassi, R. (1999) *FEBS Lett. 456*, 1−6.
19. Bassi, R., Sandona, D., and Croce, R. (1997) *Physiol. Plant. 100*, 769−779.
20. Bassi, R., Pineau, B., Dainese, P., and Marquardt, J. (1993) *Eur. J. Biochem. 212*, 297−303.
21. Horton, P., Ruban, A. V., and Walters, R. G. (1996) *Annu. Rev. Plant Physiol. Mol. Biol. 47*, 655−684.
22. Sapozhnikov, D. I., Krasovskaya, T. A., and Mayevskaya, A. N. (1957) *Dokl. Akad. Nauk 113*, 456−467.
23. Hager, A. (1980) in *Pigments in Plants* (Czygan, F.-C., Ed.) pp 57−79, Fischer, Stuttgart.
24. Yamamoto, H. Y. (1979) *Pure Appl. Chem. 51*, 639−648.
25. Demmig-Adams, B. (1990) *Biochim. Biophys. Acta 1020*, 1−24.
26. Demmig-Adams, B., and Adams, W. W., III (1993) in *Carotenoids in Photosynthesis* (Young, A. J., and Britton, G., Eds.) pp 206−251, Chapman and Hall, London.
27. Crofts, A. R., and Yerkes, C. T. (1994) *FEBS Lett. 352*, 265−270.
28. Walters, R. G., and Horton, P. (1995) in *Photosynthesis: From Light to Biosphere* (Mathis, P., Ed.) pp 299−302, Kluwer Academic Publishers, Dordrecht.
29. Pesaresi, P., Sandonà, D., Giuffra, E., and Bassi, R. (1997) *FEBS Lett. 402*, 151−156.
30. Walters, R. G., Ruban, A. V., and Horton, P. (1997) *Proc. Natl. Acad. Sci. U.S.A. 93*, 14204−14209.
31. Bergantino, E., Dainese, P., Cerovic, Z., Sechi, S., and Bassi, R. (1995) *J. Biol. Chem. 270*, 8474−8481.
32. Desamero, R. Z. B., Chynwat, V., van der Hoef, I., Jansen, F. J., Lugtenburg, J., Gosztola, D., Wasielewski, M. R., Cua, A., Bocian, D. F., and Frank, H. A. (1998) *J. Phys. Chem. 102*, 8151−8162.
33. Hayashi, H., Noguchi, T., and Tasumi, M. (1989) *Photochem. Photobiol. 49*, 337−343.
34. Trinkunas, G., Connelly, J. P., Müller, M. G., Valkunas, L., and Holzwarth, A. R. (1997) *J. Phys. Chem. B 101*, 7313−7320.
35. Zucchelli, G., Dainese, P., Jennings, R. C., Breton, J., Garlaschi, F. M., and Bassi, R. (1994) *Biochemistry 33*, 8982−8990.
36. Pagano, A., Cinque, G., and Bassi, R. (1997) *J. Biol. Chem. 273*, 17154−17161.
37. Croce, R., Cinque, G., Holzwarth, A. R., and Bassi, R. (2000) *Photosynth. Res. 64*, 221−231.
38. Cinque, G., Croce, R., and Bassi, R. (2000) *Photosynth. Res. 64*, 233−242.
39. Ide, J. P., Klug, D. R., Kühlbrandt, W., Porter, G., and Barber, J. (1986) in *Ultrafast Phenomena* (Fleming, G. R., and Siegamn, A. E., Eds.) pp 406−408, Springer, Berlin.
40. Eads, D. D., Webb, S. P., Owens, T. G., Mets, L., Alberte, R. S., and Fleming, G. R. (1987) in *International Congress on Photosynthesis* (Biggins, J., Ed.) pp 135−138, Nijhoff, Dordrecht, The Netherlands.
41. Kwa, S. L. S., Vanamerongen, H., Lin, S., Dekker, J. P., Grondelle, R. V., and Struve, W. S. (1992) *Biochim. Biophys. Acta 1102*, 202−212.
42. Nussberger, S., Dekker, J. P., Kühlbrandt, W., van Bolhuis, B. M., van Grondelle, R., and van Amerongen, H. (1994) *Biochemistry 33*, 14775−14783.
43. Savikhin, S., van Amerongen, H., Kwa, S. L. S., van Grondelle, R., and Struve, W. R. (1994) *Biophys. J. 66*, 1597−1603.
44. Du, M., Xie, X., Mets, L., and Fleming, G. R. (1994) *J. Phys. Chem. 98*, 4736−4741.
45. Bittner, T., Irrgang, K. D., Renger, G., and Wasielewski, M. R. (1994) *J. Phys. Chem. 98*, 11821−11826.
46. Bittner, T., Wiederrecht, G. P., Irrgang, K. D., Renger, G., and Wasielewski, M. R. (1995) *Chem. Phys. 194*, 311−322.
47. Peterman, E. J. G., Dukker, F. M., and van Amerongen, H. (1995) *Biophys. J. 69*, 2670−2678.
48. Peterman, E. J., Hobe, S., Calkoen, F., van Grondelle, R., Paulsen, H., and Van Amerongen, H. (1996) *Biochim. Biophys. Acta 1273*, 171−174.
49. Visser, H. M., Kleima, F. J., van Stokkum, I. H. M., van Grondelle, R., and van Amerongen, H. (1996) *Chem. Phys. 210*, 297−312.
50. Connelly, J. P., Müller, M. G., Bassi, R., Croce, R., and Holzwarth, A. R. (1997) *Biochemistry 36*, 281−287.
51. Connelly, J. P., Müller, M. G., Hucke, M., Gatzen, G., Mullineaux, C. W., Ruban, A. V., Horton, P., and Holzwarth, A. R. (1997) *J. Phys. Chem. 101B*, 1902−1909.
52. Kleima, F. J., Gradinaru, C. C., Calkoen, F., van Stokkum, I. H. M., van Grondelle, R., and van Amerongen, H. (1997) *Biochemistry 36*, 15262−15268.
53. Peterman, E. J. G., Monshouwer, G. R., van Stokkum, I. H. M., van Grondelle, R., and van Amerongen, H. (1997) *Chem. Phys. Lett. 264*, 279−284.
54. Guelen, D., van Grondelle, R., and van Amerongen, H. (1997) *J. Phys. Chem. B 101*, 7256−7261.
55. Trinkunas, G., Müller, M. G., Martin, I., Valkunas, L., and Holzwarth, A. R. (1998) in *International Congress on Photosynthesis* (Garab, G., Ed.) pp 285−288, Kluwer Academic Publishers, Dordrecht, The Netherlands.
56. Gradinaru, C. C., Ozdemir, S., Gulen, D., Van Stokkum, I. H. M., Van Grondelle, R., and Van Amerongen, H. (1998) *Biophys. J. 75*, 3064−3077.
57. Gradinaru, C. C., Pascal, A. A., van Mourik, F., Robert, B., Horton, P., van Grondelle, R., and van Amerongen, H. (1998) *Biochemistry 37*, 1143−1149.
58. Barzda, V., Peterman, E. J. G., van Grondelle, R., and van Amerongen, H. (1998) *Biochemistry 37*, 546−551.
59. Valkunas, L., Cervinskas, V., Trinkunas, G., Müller, M. G., and Holzwarth, A. R. (1998) in *International Congress on Photosynthesis* (Garab, G., Ed.) pp 281−284, Kluwer Academic Publishers, Dordrecht, The Netherlands.
60. Valkunas, L., Cervinskas, V., Trinkunas, G., Müller, M. G., and Holzwarth, A. R. (1999) *J. Chem. Phys. 111*, 3121−3132.
61. Cinque, G., Croce, R., Holzwarth, A., and Bassi, R. (2000) *Biophys. J. 79*, 1706−1717.
62. Walla, P. J., Yom, J., Krueger, B. P., and Fleming, G. R. (2000) *J. Phys. Chem. B 104*, 4799−4806.
63. Berthold, D. A., Babcock, G. T., and Yocum, C. F. (1981) *FEBS Lett. 134*, 231−234.
64. Dainese, P., Hoyer-Hansen, G., and Bassi, R. (1990) *Photochem. Photobiol. 51*, 693−703.
65. Schägger, H., and Von Jagow, G. (1987) *Anal. Biochem. 166*, 368−379.
66. Nothnagel, E. A. (1987) *Anal. Biochem. 163*, 224−237.
67. (1999), Microcal Software, Inc., Northampton, MA.
68. Ruban, A. V., Lee, P. J., Wentworth, M., Young, A. J., and Horton, P. (1999) *J. Biol. Chem. 274*, 10458−10465.
69. Bassi, R., Silvestri, M., Dainese, P., Moya, I., and Giacometti, G. (1991) *J. Photochem. Photobiol., B 9*, 335−354.
70. Rogl, H., Schödel, R., Lokstein, H., Kühlbrandt, W., and Schubert, A. (2002) *Biochemistry 41*, 2281−2287.
71. Andersson, P. O., Gillbro, T., Ferguson, L., and Cogdell, R. J. (1991) *Photochem. Photobiol. 54*, 353−360.
72. Frank, H. A., Bautista, J. A., Josue, J., Pendon, Z., Hiller, R. G., Sharples, F. P., Gosztola, D., and Wasielewski, M. R. (2000) *J. Phys. Chem. B 104*, 4569−4577.
73. Croce, R., Muller, M. G., Bassi, R., and Holzwarth, A. R. (2001) *Biophys. J. 80*, 901−915.
74. Sandonà, D., Croce, R., Pagano, A., Crimi, M., and Bassi, R. (1998) *Biochim. Biophys. Acta 1365*, 207−214.
75. Giuffra, E., Zucchelli, G., Sandona, D., Croce, R., Cugini, D., Garlaschi, F. M., Bassi, R., and Jennings, R. C. (1997) *Biochemistry 36*, 12984−12993.
76. Benfey, D. B., Brown, D. C., Davis, S. J., Piper, L. G., and Fouter, F. R. (1992) *Appl. Opt. 31*, 7034−7040.
77. Melhuish, W. H. (1962) *J. Opt. Soc. Am. 52*, 1256−1258.
78. Ruban, A. V., Phillip, D., Young, A. J., and Horton, P. (1997) *Biochemistry 36*, 7855−7859.
79. Frank, H. A., Das, S. K., Bautista, J. A., Bruce, D., Vasilev, S., Crimi, M., Croce, R., and Bassi, R. (2001) *Biochemistry 40*, 1220−1225.
80. Gradinaru, C. C., van Stokkum, I. H. M., Pascal, A. A., van Grondelle, R., and van Amerongen, H. (2000) *J. Phys. Chem. B 104*, 9330−9342.

BI0204802